International Journal of Scientific Research in Science and Technology
Print ISSN: 2395-6011 | Online ISSN: 2395-602X (www.ijsrst.com)
doi : https://doi.org/10.32628/IJSRST

Design and Implementation of Wind Turbine Integrated Generator Rectifier System with Fuzzy Logic Controller Based MPPT

MS Indiramba[1], Dr. S.Mallikarjunaiah[2]
M. Tech Student[1], Professor[2]
Department of Electrical and Electronics Engineering, VEMU Institute of Technology, P. Kothakota , Andhra Pradesh, India

Article Info
Volume 9, Issue 6
Page Number : 233-242

Publication Issue
November-December-2022

Article History
Accepted : 10 Nov 2022
Published : 25 Nov 2022

ABSTRACT

In this study, a Fuzzy Logic Controller (FLC) based Maximum Power Point Tracking (MPPT) technique is used for the design and analysis of a wind turbine integrated generator rectifier system. The proposed system will gets the power supply from the primary source known as wind power generation. Among all these renewable energy resources, the offshore wind is the rapidly growing source due to its more advantages. In this the power supply from the generator rectifier system is given to the dc grid by connecting a rectifier circuit ac power into dc power. Here two types of rectifiers are implemented active rectifier and passive rectifier. Comparatively, the passive rectifier is modelled by a controllable voltage source while the active rectifier is modelled by a controllable current source. Because of the presence of uncontrolled passive rectifiers, the deployment of generator-rectifier systems in offshore wind energy necessitates a technique known as MPPT. In the controlling topology of a generator-rectifier system, a PI controller is used to control the reference current. But by employing PI controller will leads to less speed response of the system. So, to overcome these issues, PI controller is replaced with FLC topology which improves the system performance by enhancing good speed response of the system. The simulation of this proposed work can be evaluated by using Matlab/Simulink 2018a Software.

Keywords: Wind, Inverter, Rectifier, Generator, MPPT, PI Controller, Fuzzy Logic Controller

I. INTRODUCTION

The most promising form of renewable energy remains wind turbine system (WTS) technology. They are extremely cutting-edge power plants. As proposed in [1]-[2] WTSs are frequently utilized by distribution networks, huge amount of power attaining from wind is transferred through the networks of transmission lines. WECS which are utilizing and introduced in latest times are meant to

develop to overcome the issues of more cost and boost up the energy sources. Permanent-magnet synchronous generators are a key component of the most advanced WECS designs (PMSGs). In WECSs with synchronous generators tied to a variable-speed grid, the stator and grid must have a converter interface; typically, a capacitive dc bus is employed in between the converters at grid side and stator side. As mentioned in [3]-[4], the grid codes needs the regulation of voltage and frequency by enabling the wind farm which has the controlling of reactive and real power. Moreover, the VSIs are integrated with the grid converters. The most efficient rectifiers are passive diode-bridge devices, but their dc voltage is unregulated. Rectifiers which are having active switches are used to control the voltage at the side of DC-bus but it is having more disadvantages like complexity and high losses. Design restrictions are also imposed by active switches, which are also available but have low voltage and power ratings. As proposed in [5]-[6], for meeting the requirements of power and voltage the series and parallel connected devices are employed. As mentioned in [7], the employment of MPPT can made possible for the power change. Contrary to PV systems, in the meanwhile, the irradiance will have the linear function [8], WECS torque obtained at the output side is a square function of wind speed. The irradiation must also change at a constant rate throughout the sampling period. Due to the sampling period typically being set to be equal to the settling time, a measurement taken in the middle will not accurately reflect the true value. These methods are quick and efficient, but they are system-specific and cannot be combined with variable-pitch control. The variable efficiencies of the generator-converter subsystems make it possible for the actual optimum points to differ from the stored ones even when the pitch angle is constant. Lookup-table-like techniques almost always assume that there is only one optimal curve because this phenomenon has never been studied before [8]–[10]. To implement MPPT, an approach for management that takes into account the relationship between the total dc-transport power and the dynamic rectifier's d-axis current is postulated. The elimination of capacitors which are used as filters at the outputs of passive-rectifier. In the process of reducing the ripples obtained in the voltage at the dc-bus the adjustment of corresponding phases. In this study, the power controller of the integrated generator-rectifier system receives PI controlling signals. in the controlling topology. The system responds slowly and exhibits more harmonic distortions when a PI controller is used, though. The PI controller is swapped out for a Fuzzy Logic Controller to address these issues. They are easier to customize in natural language terms, cover a wider range of operating conditions, and are less expensive to develop. The system's power quality and speed response both increase as a result of the implementation of this FLC. The system description is shown in Section-II, the proposed controlling topology is explained in Section-III, and the results and discussion are covered in Section-IV. Section-I describes the introduction and literature review. The completion of this work brings Section V to a close.

II. DESCRIPTION OF THE SYSTEM

The wind turbine power-point tracking architecture uses a wind turbine with variable speed as its primary motor. An internal shaft connects the multiport PMSG and the turbine. Direct current (DC) is produced by a generator-rectifier system that is integrated (DC). A connection is made between the dc output and the rigid interface at dc side. To control the extraction of maximum power is monitored by the proposed system. A three-phase ac port is signified by a back EMF source coupled in series with the phase resistance R and inductance L of a generator. In contrast to the active rectifier, which is a 3-phase, 2-level converter, the passive rectifier uses a diode rectifier with six pulses.

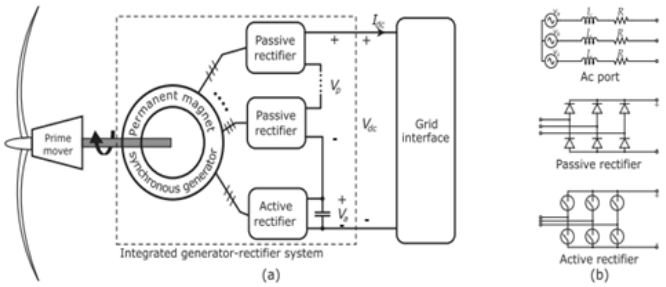

Figure 1 : Schematic Representation of Proposed System

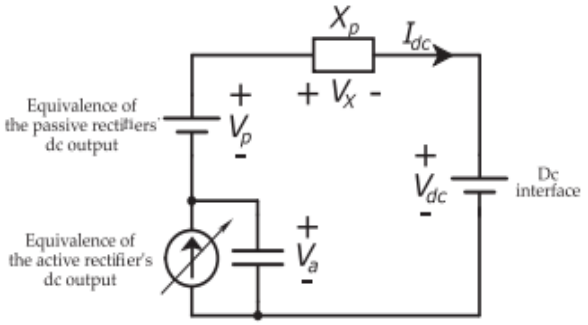

Figure 2 : Generator rectifier system's equivalent circuit

A) Generator rectifier systems power flow control:

In this, the development of the proposed system which controls the flow of power related architecture is depicted. The output obtained at the dc side is connected to the dc side which is rigid. This topology is supported by using the collection of both dc and ac related grids. In the case of AC the converter at the grid side will acts as the interface to control the dc bus which is used as an intermediate. At the same time, the voltage at the DC side can be controlled by the converter which is placed in the dc-grid substation. In Figure 2, the integrated system's condensed equivalent circuit is depicted. To simulate the overall output of the passive rectifiers, link a commutation reactance (Xp) in series with a voltage source with generator speed dependence (Vp). By making sure that there is a phase shift between the various ac ports, as explained in Section II-B, the ignorance of ripples occurred in the voltage can be possible here. The difference between the output voltage of a passive rectifier and the constant grid interface voltage, denoted by the notation Vdc, is referred to as the active-rectifier voltage at dc-side or Va. The active rectifier's dc-side current depends on the amount of controllable power it consumes. A controllable current source simulates the active rectifier. According to Section II-C, the series connection causes the amount of power entering the dc bus to depend on the current leaving the active rectifier. It is advised to use cascading PI controllers in practical applications. However, in this work a fuzzy logic controller replaces the PI controller. To implement MPPT, Section II-D makes use of the power-flow control framework.

B. Passive-Rectifier Voltage-Ripple Minimization:

Without utilizing the capacitive filters, a pmsg machine which is built up with k 3-phase ac ports is enough for each passive rectifier. When its dc output voltage ripple peaks every k1/3 radians. With the appropriate phase shift and connection of outputs obtained at the dc side will calculate the ripples attained at the peak-to-peak position. Two passive rectifiers, for instance, have a ripple percentage of 3% 6% phase shifting instead of 14% without it. In a system with (k1) passive rectifiers, a 3(k1) radian phase shift lowers voltage ripple. The percentage of voltage ripple is decreased by adding more ac ports, but at a decreasing rate (c). This method is comparable to how phase shifting transformers and multi-pulse diode rectifiers in drives which are highly powered will reduce the distortions obtained in the line currents. The voltage frequency obtained at the passive rectifier side will depicted as follows.

$$\boldsymbol{V_{passive}} = \frac{3}{\pi}(\boldsymbol{k-1})\sqrt{\boldsymbol{3E(\omega)}} - (\boldsymbol{k-1})(\frac{3}{\pi}\boldsymbol{\omega L} + \boldsymbol{2R})\boldsymbol{I_{dc}} \quad (1)$$

In this the AC port's equivalent series resistance and synchronous inductance for each phase are depicted with L and R and the back emf which is dependent on electrical frequency is depicted with E(ω).

$$\mathbf{E}\,(\boldsymbol{\omega}) = \frac{\boldsymbol{\omega}}{\boldsymbol{2\pi f_0}}\boldsymbol{E_0} \quad (2)$$

AC port which is Each ac port is designated by its electrical frequency, or f0, and its rated line-to-neutral peak back EMF, or E0. The dc-side voltage of a passive rectifier is influenced by the inductance which is synchronized, phase resistance, and dc-bus current. These outcomes are all a part of VX. In order to this for a typical six-pulse diode bridge rectifier to operate in Mode I, which corresponds to

commutation obtained in the phase current lasting less than 1/6th of the electrical period, it is presumable that the synchronous inductance of the device is sufficiently low.

C. Implementation of Active rectifier to control power flow: to establish a connection in between the active rectifier's dc bus power and ac side current. In case of neglecting the losses occurred in the conversion process the balancing of power can be obtained at the sides of ac and dc.

$$\frac{3}{2}\boldsymbol{E(\omega)I_{sd}} - \frac{3}{2}\boldsymbol{I_{sd}^2 R} = \boldsymbol{V_a I_{dc}} \quad (3)$$

The voltage and current at dc-side of active rectifier is depicted with Va and Isd. This related equation is depicted below.

$$\boldsymbol{V_a = V_{dc} - V_p + X_p I_{dc}} \quad (4)$$

The current obtained at dc-bus side is represented by,

$$I_{dc} = \frac{P_{dc}}{V_{dc}} \quad (5)$$

The power at dc bus side is depicted with Pdc. When combining equations 3, 4 and 5 the below euq-6 is obtained.

$$\frac{3}{2}E(\omega)I_{sd} - \frac{3}{2}I_{sc}^2 R = P_{dc}^2\left((k-1)\frac{1}{V_{dc}^2}\left(\frac{3}{\pi}\omega L + 2R\right)\right) + P_{dc}\left(1 - \frac{3}{\pi}(k-1)\frac{\sqrt{3E(\omega)}}{V_{dc}}\right) \quad (6)$$

The above equ-6 will defines how the entering and leaving of power is attained from the turbine and the controlling of d-axis current of an active-rectifier.

As depicted in fig-5, the flow of power will be regulated by the cascaded architecture. The currents of d and q axis attained at the side of rectifier will be regulated by the current controllers presented in the inner loop. These axis related currents will regulate the flow of power and power factor. The calculation of current obtained at d-axis will leads to the control of outer power loop by the deliverance of reference power Pdc. The command of power is generated by an MPPT technique using the revolving speed of the generator as an input. The current of q-axis is exactly opposite to the current of active rectifier (Iq=0, Iar=1). The dynamics of ac-port currents in the provided dq reference frame serve as the foundation for the current controllers.

$$L\frac{dI_{SD}}{dt} = -RI_{sd} + \omega LI_{sq} + E - V_{rd} \quad and \quad (7)$$

$$L\frac{dI_{Sq}}{dt} = -RI_{sq} + \omega LI_{sd} + E - V_{rq} \quad (8)$$

The d and q-axis input voltages are Vrd and Vrq, respectively. The parallel connection is there in between the back emf and d-axis. The q-axis and the d-axis are parallel. The below equation is depicting the feedforward terms and voltage at the d-axis

$$V_{rd}^* = K_{pi}(I_{sd}^* - I_{sd}) + \int K_{ii}(I_{sd}^* - I_{sd})dt + E + \omega_0 LI_{sq} \quad (9)$$

Where the proportional gain, d-axis reference current and integral gain is denoted by using I *sd, Kip, and Kii respectively. In the similar manner the reference current is depicted.

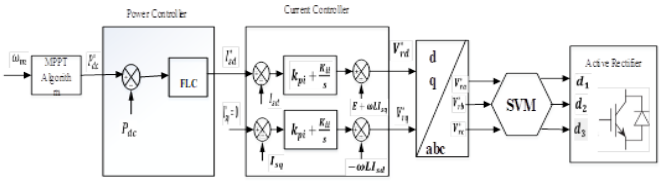

Figure 3. Controlling topology of proposed system

The current obtained at the d-axis can be calculated directly to achieve the demand of power. The uncertainties obtained at the time of controlling the flow of power. This related equation is employed below.

$$\boldsymbol{I_{sd}^* = K_{pp}(P_{dc}^* - P_{dc}) + K_{ip}\int (P_{dc}^* - P_{dc})dt} \quad (10)$$

Where proportional and integral gains are denoted by using Kpp and Kip

D. Employing MPPT based technique in Generator-Rectifier system:

The peak power point of the wind turbines is monitored using the proposed controlling topology

utilized. For MPPT to work, the curve of maximum power at each generator speed must be adhered. Consider the operation in a windy environment with a 12 m/s wind speed. So, a 10MW of power is extracted.

III. PROPOSED FUZZY LOGIC CONTROLLER

(FLC), which operates based on logical rules formed by input and output arguments. And also it converts crisp values to fuzzy values (analog to logical). It is implemented by using the membership functions. The FLC system mainly compresses of 4 major parts known as fuzzification (converts fuzzy sets to crisp sets), rules base, inference engine and defuzzification (crisp sets to fuzzy sets) that can be depicted in below figure-4.

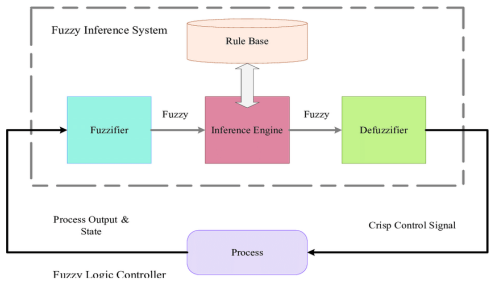

Figure 4 : Schematic diagram of FLC

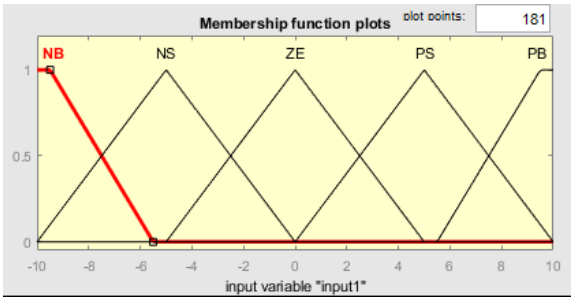

Figure 5 : Power Error

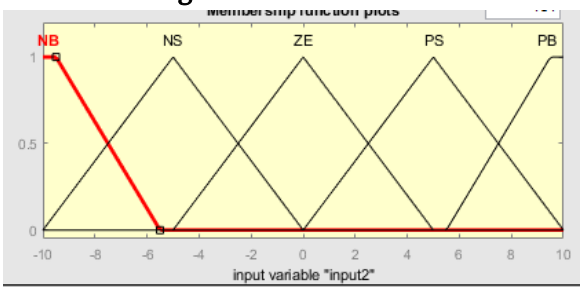

Figure 6 : Power Change in error

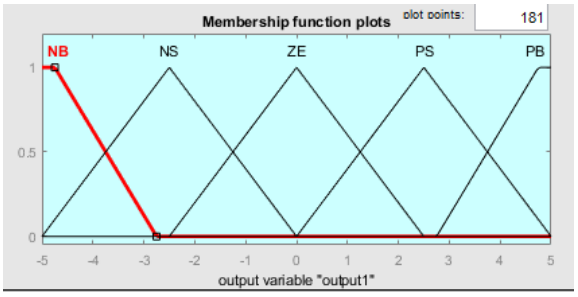

Figure 7 : Id Current reference

The PI Controller in the controlling topology is replaced with Fuzzy logic controller. The FLC is placed in the power controller. The power (Pdc) and power error (P*dc) is given as inputs as shown in the figure 5 and 6, to the FLC to regulate the reference currents which is depicted in figure-7. The rules that are implemented in this work is depicted in below table-1.

Table 1: Rules table

E/CE	NB	NS	ZE	PS	PB
NB	ZE	NS	NB	NB	NB
NS	ZE	NS	NB	NS	NB
ZE	PB	PS	ZE	NS	NB
PS	PB	PS	PS	ZE	NS
PB	PB	PB	PB	PS	ZE

IV. RESULTS AND DISCUSSION

The simulation results that were obtained using both PI and a FLC are shown in this section. The 2018a version of Matlab/Simulink is used to validate the simulation results.

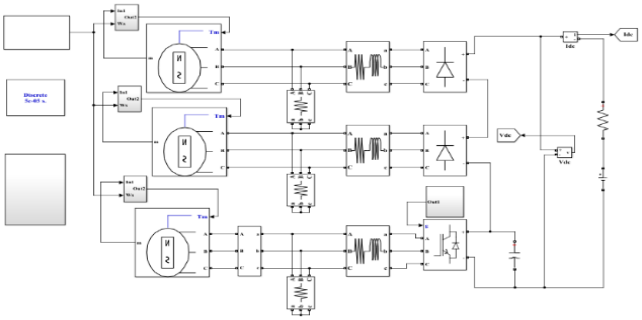

Figure 8 : Simulation Model of proposed system

The above figure will depicts about the simulink of the proposed system employed at different generating

speeds which uses a PMSG integrated with different Power devices. The designing of simulink model is implemented to attain the relation between the d-axis related currents and power obtained at the dc bus. Three series-connected voltage sources with resistance and inductance are used to simulate a three-port PMSG. The assumed signal of reference speed will measure the voltage and frequency in the system. The specified values are used to set the port's parameters. Three-phase diode rectifiers are connected to ports 1-2. The phase-A voltages of these two ports, along with the Phase-B and -C voltages, are spaced apart by $\pi/6$ electrical radians in order to reduce ripples occurred in the voltage on the dc output of passive rectifier. Port 3 supplies power to a 2 kHz active rectifier based on an insulated-gate bipolar transistor (IGBT). The formation of dc bus will be obtained by connecting the outputs of rectifier in series connection.

a) Simulation Results obtained by using PI Controller

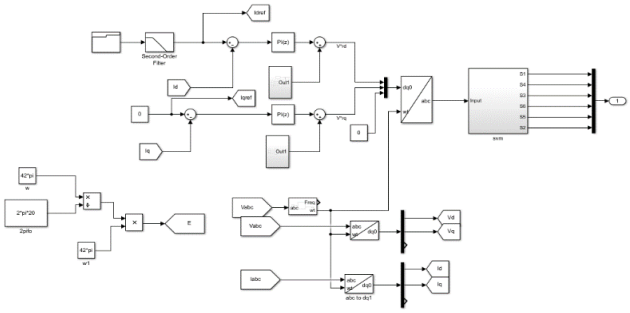

Figure-9 : Simulink model of PI Controller employed in controlling topology

The above figure will depicts about the simulink model of the controlling topology employed PI controller in the power controller terminology to regulate the reference current (Idc*).

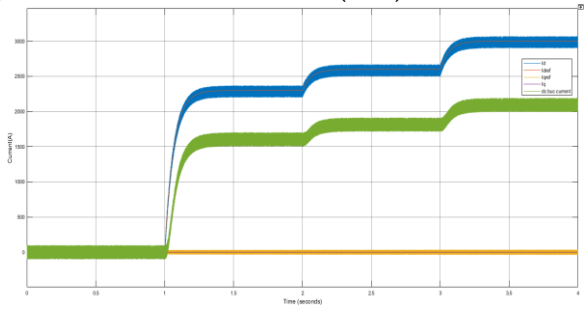

Current

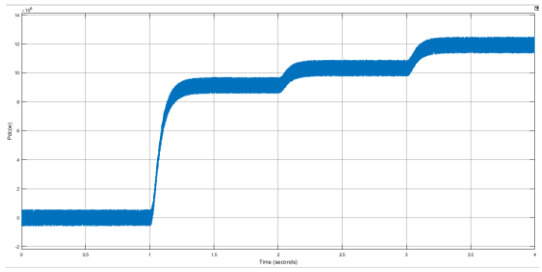

Dc power

Fig 10

The d-axis current of active rectifier system is depicted in Figure 10 as the dc-bus power's control input. The above fig depicts the waveforms of currents which are corresponding to the reference currents related to d-axis of the active rectifier when it is instructed for the Iq=0. Dc-bus current is the name given to the current that comes after the d-axis current.

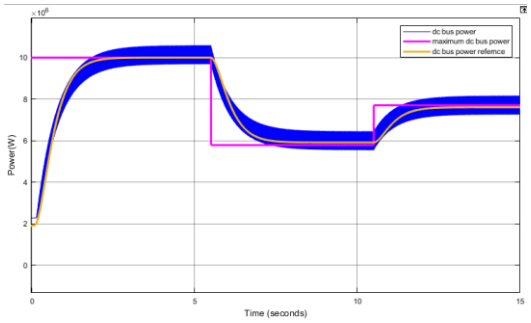

Power

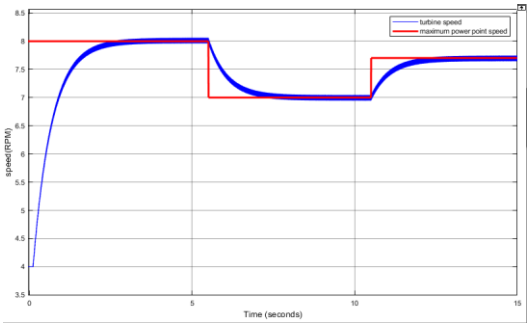

Speed

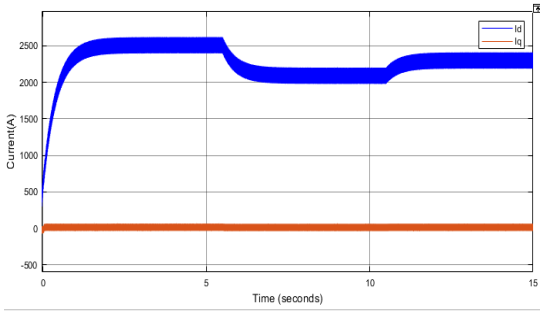

Current

Figure 11. The above figure will depicts about the simulation results obtained to illustrate the capability of MPPT technique. The current and speed related

waveforms are depicted with respect to their reference currents and speeds.

At W=40π

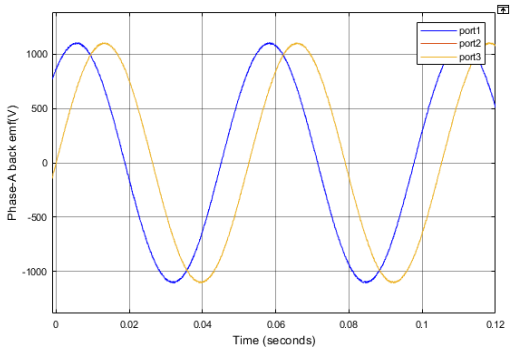

(a) At rated speed of generator the obtained back emfs

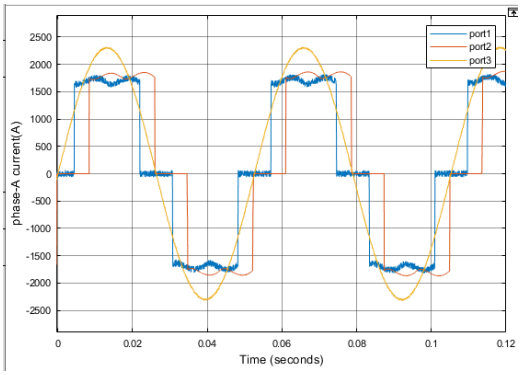

(b) Currents obtained at phase-A.

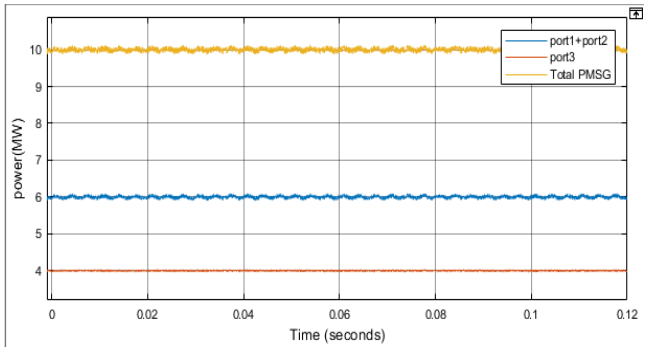

(c) Reactive Vs Active power based Input power

At, speed=40π, the above figures a, b and c related results are obtained. In figure (a), the obtained back emf is obtained. It is in sinusoidal form with an amplitude of 1100v (app). Whereas figure (b) depicts about the corresponding currents obtained based on speed. Almost port-1 and port-2 currents have attained with same amplitude but the waveform of current at port-3 is in sinusoidal from. The power-related results are shown in figure (c).

Total power is obtained by calculating the electrical output of all back emf sources.

At W=22π

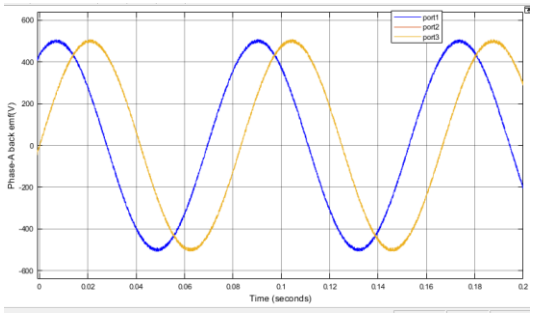

d) At 55% rated the obtained back emf curve

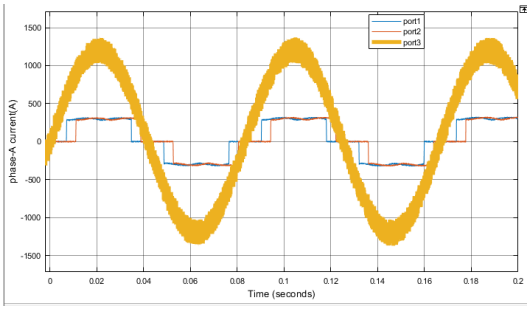

e) The curve of currents obtained at minimum speed in phase-A

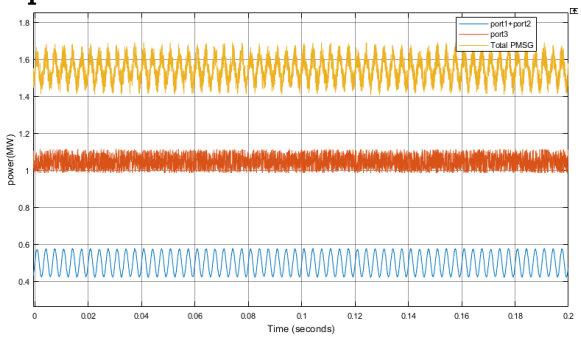

f) Figure showing the sharing of active and reactive power obtained at minimum speed

The above figures d, e and f results are obtained at the operating speed of 55%. In the figure (d) the amplitude and frequency of back emf is proportional to speed of the generator. As shown figure (e), the ports of AC currents will be varied for delivering the power depicted in figure (e).

A. Simulation results using FLC:

In this section, the FLC controller based simulation results are evaluated over here. The simulation diagram of this method is depicted below and the related results are shown below.

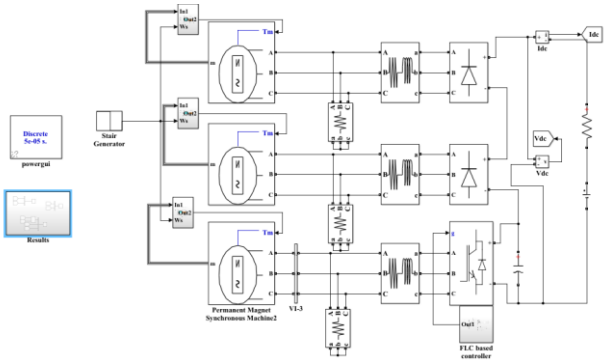

Figure 12: FLC based Simulation diagram

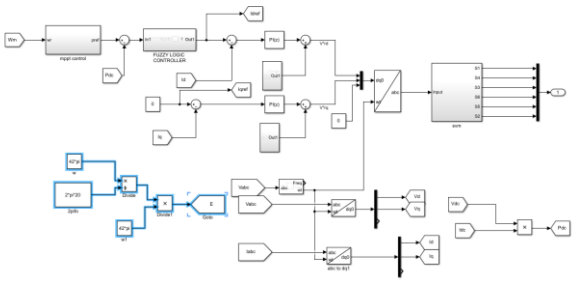

Figure 13 : FLC based Controlling topology

The above figure will depicts about the implementation of FLC in power controller to regulate the reference currents. This related results are depicted below.

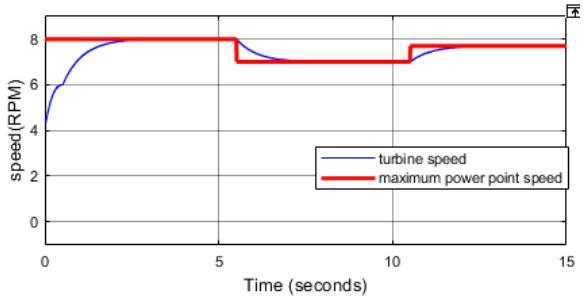

a) Turbine speed Vs MPPT speed

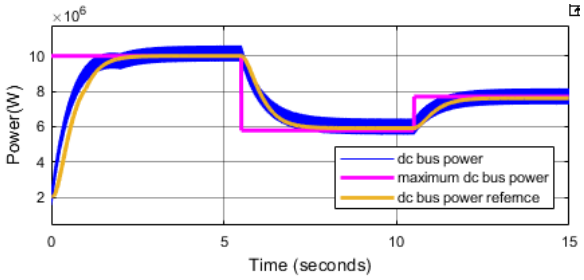

(b) Power of DC Bus and mechanical turbine Vs Time

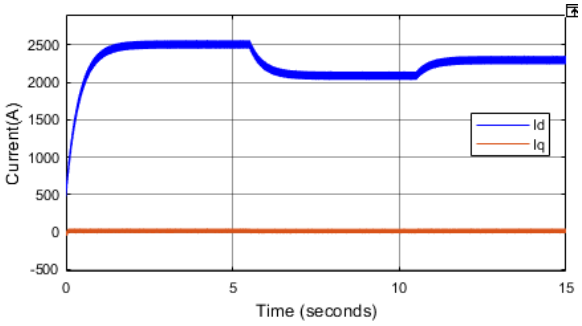

(C) To attain MPPT at Id and Iq

The above figure-a will depicts about the reference currents obtained. The q-axis current is equals to zero, whereas d-axis current amplitudes has changed with respect to the time. In figure (b) the speed of the turbine has varied by changing the speed of maximum power point tracking.

At w=40pi (rad/sec)

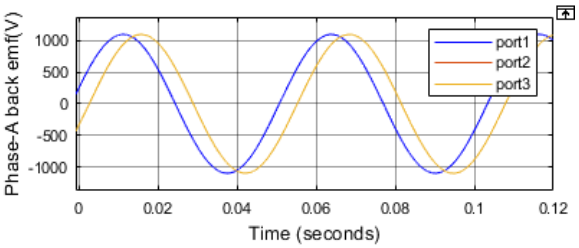

a) At rated generated speed the obtained back emf

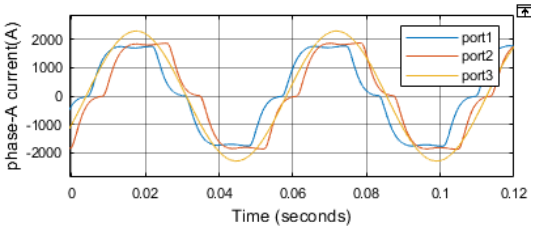

b) Currents obtained in phase-A

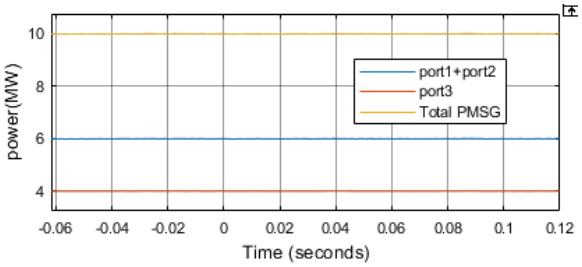

C) Reactive Vs Active power based Input power

At w=22pi (rad/sec)

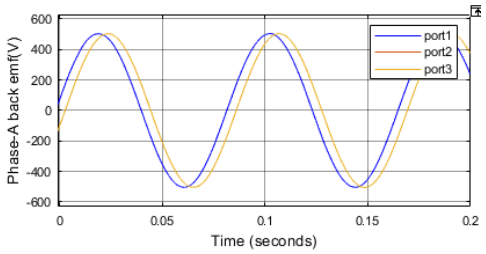

d) Obtained back emf

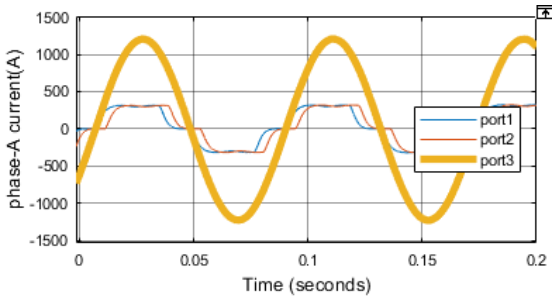

e) Obtained phase-A currents

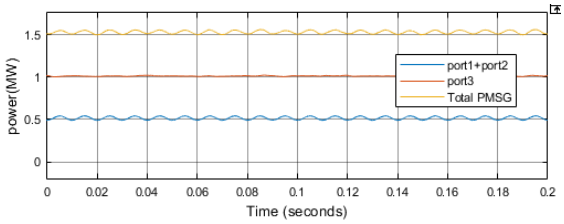

F) Figure showing the sharing of active and reactive power obtained at minimum speed

The above figure will depicts about the FLC based results at w=22pi, the obtained back emf, sharing of active and reactive power and the currents in Phase-A

V. CONCLUSION

The design and Implementation of Wind Turbine Integrated Generator Rectifier System with Fuzzy Logic Controller Based MPPT is implemented in this work. A new technique known as Fuzzy Logic Controller based MPPT was employed. The power obtained from generator rectifier system was given to the dc grid. In the rectifier system mainly two components are used namely active rectifier and passive rectifier. They were modelled with respective current and voltage sources. Then the converted power is given to the DC grids. In the MPPT technique the power controller is controlled by using conventional topology known as PI controller. But this PI controlled has less speed response of the system. To overcome this, the PI controller is replaced with FLC. This has improved the system performance and also the speed response of this generator-rectifier system is increased. The simulation results of this system was evaluated by using Matlab/Simulink 2018a Software.

VI. REFERENCES

[1]. M. Liserre, R. Cardenas, M. Molinas, and J. Rodriguez, "Overview of multi-MW wind turbines and wind parks," IEEE Trans. Ind. Electron., vol. 58, no. 4, pp. 1081–1095, Apr. 2011.

[2]. Z. Chen, J. M. Guerrero, and F. Blaabjerg, "A review of the state of the art of power electronics for wind turbines," IEEE Trans. Power Electron., vol. 24, no. 8, pp. 1859–1875, Aug. 2009.

[3]. S. M. Muyeen, R. Takahashi, T. Murata, and J. Tamura, "A variable speed wind turbine control strategy to meet wind farm grid code requirements," IEEE Trans. Power Syst., vol. 25, no. 1, pp. 331–340, Feb. 2010.

[4]. Z. Chen and E. Spooner, "Current source thyristor inverter and its active compensation system," Proc. Inst. Elect. Eng.—Gener. Transm. Distrib., vol. 150, no. 4, pp. 447–454, Jul. 2003.

[5]. J. Rodriguez, S. Bernet, B. Wu, J. O. Pontt, and S. Kouro, "Multilevel voltage-source-converter topologies for industrial medium-voltage drives," IEEE Transactions on Industrial Electronics, vol. 54, no. 6, pp. 2930–2945, Dec 2007.

[6]. F. Blaabjerg, M. Liserre, and K. Ma, "Power electronics converters for wind turbine systems," IEEE Transactions on Industry Applications, vol. 48, no. 2, pp. 708–719, March 2012.

[7]. D. Sera, R. Teodorescu, J. Hantschel, and M. Knoll, "Optimized maximum power point tracker for fast-changing environmental conditions," IEEE Trans. Ind. Electron., vol. 55, no. 7, pp. 2629–2637, Jul. 2008.

[8]. R. Cardenas, R. Pena, M. Perez, J. Clare, G. Asher, and P. Wheeler, "Control of a switched reluctance generator for variable-speed wind energy applications," IEEE Trans. Energy Convers., vol. 20, no. 4, pp. 781–791, Dec. 2005.

[9]. Q. Wang and L. Chang, "An intelligent maximum power extraction algorithm for inverter-based variable speed wind turbine systems," IEEE Trans. Power Electron., vol. 19, no. 5, pp. 1242–1249, Sep. 2004.

[10]. C.-T. Pan and Y.-L. Juan, "A novel sensorless MPPT controller for a high-efficiency microscale wind power generation system," IEEE Trans. Energy Convers., vol. 25, no. 1, pp. 207–216, Mar. 2010.

Cite this article as :

MS Indiramba, Dr. S. Mallikarjunaiah, "Design and Implementation of Wind Turbine Integrated Generator Rectifier System with Fuzzy Logic Controller Based MPPT", International Journal of Scientific Research in Science and Technology (IJSRST), Online ISSN : 2395-602X, Print ISSN : 2395-6011, Volume 9 Issue 6, pp. 233-242, November-December 2022.
Journal URL : https://ijsrst.com/IJSRST229637